Desalination and Water Treatment
www.deswater.com
1944-3994 / 1944-3986 © 2011 Desalination Publications. All rights reserved.
doi: 10.5004/dwt.2011.2392

31 (2011) 54–58
July

Effect of the concentration polarization on the fouling driving force of UF membranes

Sonia Vulf, Iris Sutzkover-Gutman, David Hasson*, Raphael Semiat

Rabin Desalination Laboratory, Grand Water Research Institute, Department of Chemical Engineering, Technion–Israel Institute of Technology, Haifa 32000, Israel
Tel. +972 (4) 829-2936; Fax +972 (4) 8295672; email: hasson@tx.technion.ac.il

Received 11 October 2010; Accepted 2 December 2010

ABSTRACT

The main objective of this work was to investigate the effect of foulant concentration prevailing at the membrane surface on the rate of flux decline. The significant role of foulant membrane concentration was highlighted by analysis of the well-known filtration blocking laws. All blocking mechanisms were found to predict that the initial fouling rate depends on the product of feed concentration and initial permeate flow rate. Humic acid fouling data were analyzed to provide values of the fouling rate dJ_v/dt vs. membrane surface concentration C_m. The data of all runs, covering a rather broad range of conditions, fell within a narrow band thus supporting the contention that foulant concentration on the membrane is one of the main parameters governing the fouling rate.

Keywords: UF membrane; Fouling; Concentration polarization; Critical flux; Humic acid

1. Introduction

Membranes play a major role in industrial practice due to their conspicuous advantages relative to other separation techniques. They are usefully applied in processes involving concentration, purification and solute separations [1]. The main difficulty encountered in membrane operation is related to fouling and concentration polarization [CP] problems [2]. Membrane fouling involves accumulation of a deposit on the membrane surface and inside membrane pores. Fouling may take several forms: adsorption, pore blockage, deposit or gel formation induced by the CP effect. The flow resistances imposed by the deposits lead to a decline in permeate flux [3].

The concentration polarization phenomenon is commonly analyzed by the film theory. According to this theory, the enhanced solute concentration C_m on the membrane is related to the bulk solution concentration C_b, the permeate concentration C_p and the concentration polarization (CP) modulus by [3]:

$$\frac{C_m - C_p}{C_b - C_p} = CP = e^{J_v/k} \tag{1}$$

where J_v is the flux and k is the mass transfer coefficient which is governed by the flow hydrodynamics [1]. Reduction of the CP level is known to reduce the fouling severity [4].

The "critical flux" (CF) concept [2], first suggested by Field and Howell et al. [5], stipulates the existence of a flux level below which no significant fouling is anticipated. The critical flux phenomenon has been mainly observed in micro-filtration (MF) systems, operated in cross flow with a variety of colloidal particles such as proteins, activated sludge and bacteria [5–12]. One of the techniques used to determine the critical flux is to perform constant permeate flux runs and to monitor the pressure increase

* Corresponding author.

Presented at EuroMed 2010 — Desalination for Clean Water and Energy: Cooperation among Mediterranean Countries of Europe and MENA Region, 3–7 October 2010, David Intercontinental Hotel, Tel Aviv, Israel. Organized by the European Desalination Society.

required to compensate for an induced fouling resistance. The CF is determined by noting the flux below which there is no pressure increase and the transmembrane pressure remains constant with time [13].

The mechanisms inhibiting fouling at the CF threshold are not well understood. Studies show that the magnitude of the CF level is influenced by several parameters. In general, parameters affecting the CF usually also influence the concentration polarization. Cross flow velocity and particle concentration seem to be the main parameters affecting the CF level. Increase of flow velocity augments the CF while increase of the suspension concentration lowers the CF [5–10, 14]. The lack of sufficient understanding of the critical flux phenomenon has been recently expressed by the statement "since fouling occurred irrespective of the actual flux, the critical flux concept stating that below a critical flux no fouling occurs is not a suitable approach to control biofouling of spiral wound, reverse osmosis and nanofiltration membranes" [15].

The literature referring to the critical flux concept give insufficient attention to the nature of the driving forces guiding fouling processes. It is reasonable to assume that one of the major parameters affecting the fouling rate is the foulant concentration C_m prevailing on the membrane surface as expressed by Eq. (1).

The need to consider the driving force prevailing on the membrane is also justified by our theoretical analysis of the well-known filtration blocking laws. Table 1 presents theoretical analyses of fouling rates according to the four blocking laws. All blocking mechanisms are seen to predict that the initial fouling rate depends on the product of feed concentration and initial permeate flow rate squared. It is thus very likely that increase in feed concentration aggravates fouling and therefore reduces the critical flux level, as was observed in several studies [4,14,16].

The main objective of this work was to investigate the effect of the foulant concentration prevailing at the membrane surface on the rate of flux decline in a UF system.

2. Experimental

2.1. Experimental system

Experiments were conducted in a continuous flow, tubular system (12.5 mm in diameter, 600 mm long) shown in Fig. 1. Two membranes were held in series inside an ITT PCI LTD stainless steel membrane housing, type MIC-RO 240. The membrane material was polyvinylidene

Table 1
Analyses of the driving force for fouling according to various filtration blocking mechanisms

n	Fouling mechanism	Flow rate	Fouling rate	Initial Fouling rate
0	Cake filtration	$Q=\frac{dV}{dt}=\frac{Q_o}{\sqrt{1+\frac{2\alpha Q_o}{A_o R_{mo}}\cdot ct}}$ Q = filtrate flow rate, Q_0 = initial filtration flow rate; V = filtrate volume, t = time	$-\frac{dQ}{dt}=\frac{cQ_o^2\cdot\frac{\alpha}{A_o R_{mo}}}{\left[1+\frac{2\alpha Q_o}{A_o R_{mo}}\cdot ct\right]^{1.5}}$	$-\left(\frac{dQ}{dt}\right)_{t=0}=\frac{\alpha}{A_o R_{mo}}\cdot cQ_o^{\,2}$ c = deposit vol. per unit filtration volume; A_0 = total membrane area; α = specific cake resistance; R_{mo} = membrane flow resistance
1	Intermediate law	$Q=\frac{dV}{dt}=\frac{Q_o}{\left[1+\frac{Q_o}{S_o}\cdot\sigma t\right]}$	$-\frac{dQ}{dt}=\frac{\sigma Q_o^2\cdot\frac{1}{S_o}}{\left[1+\frac{Q_o}{S_o}\cdot\sigma t\right]^2}$	$-\left(\frac{dQ}{dt}\right)_{t=0}=\frac{1}{S_o}\cdot\sigma Q_o^2$ σ = blocked area per unit filtration volume; S_o = initial pore covered surface
1.5	Standard law	$Q=\frac{dV}{dt}=\frac{Q_o}{\left[1+\frac{Q_o t}{V_{\max}}\right]^2}$	$-\frac{dQ}{dt}=\frac{cQ_o^2\cdot\frac{2}{v_o N_o A_o}}{\left[1+\frac{Q_o}{v_o N_o A_o}\cdot ct\right]^3}$	$-\left(\frac{dQ}{dt}\right)_{t=0}=\frac{2}{v_o N_o A_o}\cdot cQ_o^2$ N_o = no. of capillary pores per unit membrane area; vo = initial capillary pore volume
2	Complete blocking	$Q=\frac{dV}{dt}=Q_o\cdot\exp\left[-\frac{Q_o t}{V_{\max}}\right]$	$-\frac{dQ}{dt}=\frac{n_o Q_o^2\cdot\frac{1}{N_o A_o}}{\exp\left[\frac{Q_o}{N_o A_o}\cdot n_o t\right]}$	$-\left(\frac{dQ}{dt}\right)_{t=0}=n_o\cdot\frac{Q_o^2}{A_o N_o}$ n_o = no. of particles per unit filtration volume

fluoride and the membrane MWCO was 20 kDa. The initial permeability of a membrane varied in the range of 119–301 L/h·bar·m^2 depending on the membrane age. The experimental system was operated in a recycle mode (both permeate and concentrate returned to the feed vessel). The duration of each run was 1–2 h.

2.2. Feed solution

The foulant used was commercial humic acid. Humic substances are heterogeneous mixtures of degradation products from plant and animal residues that can dissolve in natural surface waters [17]. Humic acid (HA) is the major component of natural organic matter (NOM) found in both surface and well waters.

Humic acid solutions were prepared in the 15 L feed tank by dissolving in distilled water pre-weighed amounts of powdered humic acid, supplied by Sigma-Aldrich Chemie GmbH, Germany. The HA solutions were dosed with 0.04% (w/w) sodium azide so as to prevent microbial fouling. The solutions were stirred for 30 min in order to gain stable particle sizes of 250–350 nm. The final feed solution was set to a pH of 7 using dilute NaOH and HCl reagents.

2.3. Run procedure

The fouling experiments were carried out at constant pressure. The permeate flux decline generated by the fouling of the membrane was monitored by periodic measurements of flux. After each experiment, the membrane was cleaned by recycling a soap solution containing NaOH. Humic acid passage through the membrane was relatively constant and varied in the range of 25–35%.

2.4. Method of analysis

The concentration polarization level in each run was evaluated from Eq. (1). Flow conditions in all runs were in the turbulent region and the mass transfer coefficient k was evaluated by the Sherwood correlation [1]:

$$\mathrm{Sh} = \frac{k \cdot d}{D} = 0.023 \cdot \mathrm{Re}^{0.875} \cdot \mathrm{Sc}^{0.25} \tag{2}$$

where Sh is the Sherwood number, Re is the Reynolds number, Sc is the Schmidt number, d is the tube diameter and D is the solute diffusion coefficient. A literature search indicates that the most reliable value for the HA diffusion coefficient at room temperature is 3×10^{-6} cm^2/s [18].

Eq. (1) shows that increase of the flux level augments the concentration polarization modulus leading to enhancement of the concentration on the membrane surface. Thus, increase of the flux level can be expected to increase the intensity of flux decline.

Fouling rates were determined by fitting the flux decline data to the correlating equation developed by Probstein et al. [19]:

$$\left(J_o - J_t\right) = \left(J_o - J_t^*\right)\left(1 - e^{-t/\tau}\right) \tag{3}$$

where J_o, J_t and J_t^* are the initial, instantaneous and asymptotic fluxes, respectively and τ is a characteristic of the film build-up time. The good fit of the fouling data to this equation minimized the error involved in differentiating the experimental flux decline curve.

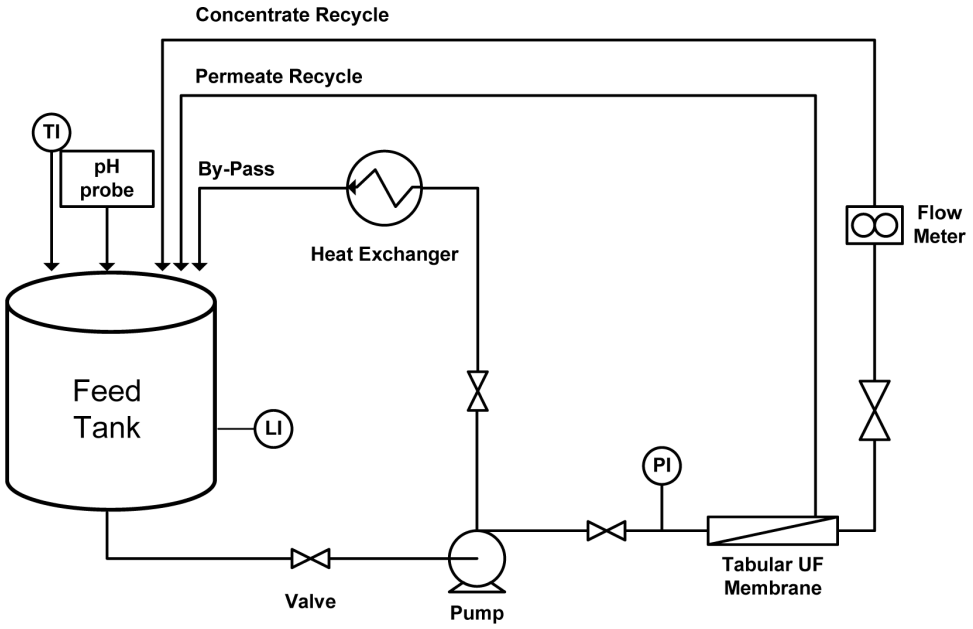

Fig. 1. Continuous flow UF system (TI – temperature indicator, PI – pressure indicator, LI – level indicator).

3. Results and discussion

The operating conditions of the experimental fouling runs (Table 2) covered a rather wide range: cross flow velocities of 50–120 cm/s, bulk HA concentrations of 5–50 ppm and initial fluxes of 2.5×10^{-3}–7.1×10^{-3} cm/s (90–260 lmh). Fig. 2 illustrates a typical flux decline curve measured in run HA8b. Fig. 3 displays the good fit obtained in plotting the flux decline data according to the linear relationship predicted by Eq. (3).

Fig. 4 shows rates of flux decline extracted from all runs vs. the humic acid concentration prevailing on the membrane surface [Eq. (1)]. As may be anticipated, there is a consistent trend of an increase in the flux decline rate as the HA membrane surface concentration is enhanced. Data points taken from experiments covering a rather wide range of conditions are seen to fall within a narrow band. Similar trends were observed in analysis of some flux decline data reported by Rubia et al. [20] who filtered HA solutions through a tubular ceramic membrane.

An interesting observation is that measurements observed in this study indicate that considerably higher levels of the CP modulus, in the range of 5–50, are encountered in UF systems, in contrast to the very low values in RO and NF systems. This observation which has an impact on fouling propensity is not sufficiently emphasized in the UF literature.

4. Concluding remarks

The main contributions of this study lie in highlighting the role of foulant concentration on the membrane surface as one of the important fouling driving force parameters and in disclosing the possibility of sustaining high concentration polarization levels in UF operations. Extension of these results can lead to improved techniques for reliable correlation of fouling data.

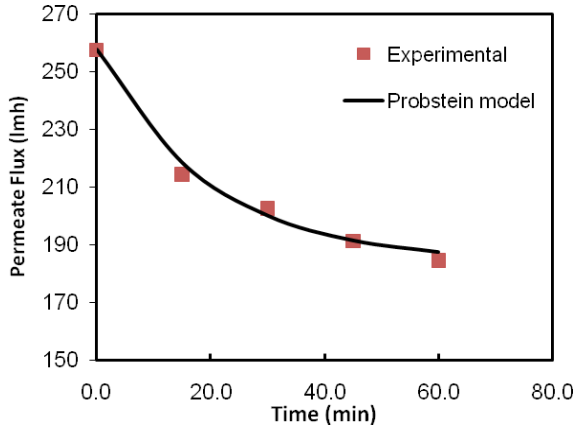

Fig. 2. Flux decline as a function of time (Run HA8b).

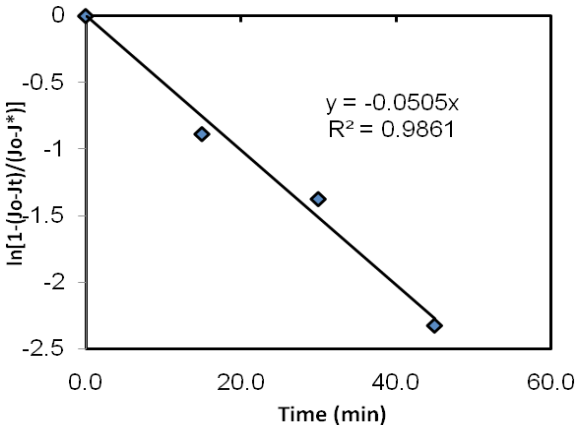

Fig. 3. Linear correlation of Run HA8b data according to Eq. (3).

Table 2
Initial operating conditions

Run No.	Feed conc. (ppm)	Mass transfer coeff. (cm/s)	Initial permeate flux (cm/s)	Flow velocity (cm/s)	Initial CP level	C_m (ppm)
HA2	20	9.79E-04	2.76E-03	56.5	16.8	240.5
HA7	50	9.02E-04	2.53E-03	51.5	16.4	590.6
HA8	10	1.48E-03	6.52E-03	90.6	82.0	577.3
HA8b	10	1.48E-03	7.15E-03	90.6	125.9	884.0
HA9	20	1.77E-03	6.07E-03	111.5	30.6	435.0
HA9b	20	1.77E-03	7.07E-03	111.5	53.8	758.6
HA10	5	1.89E-03	6.64E-03	119.8	33.7	119.3
HA11	20	1.72E-03	2.97E-03	107.6	5.6	84.9
HA13	15	1.32E-03	2.95E-03	79.3	9.4	103.0
HA14	30	8.88E-04	2.95E-03	50.5	27.7	590.4

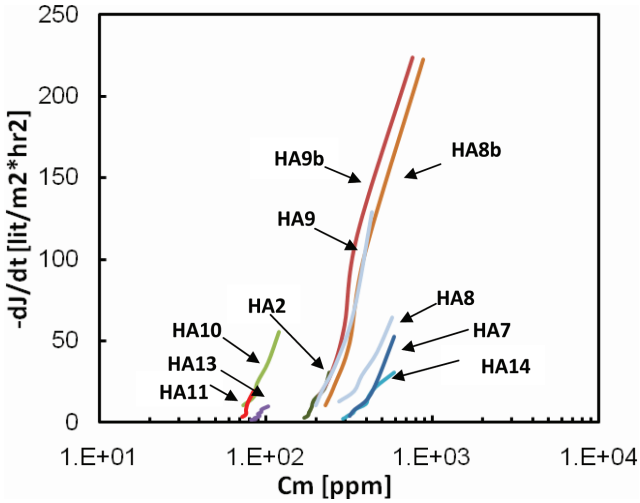

Fig. 4. Rate of flux decline vs. HA membrane surface concentration.

References

[1] M. Mulder, Basic Principles of Membrane Technology, Kluwer Academic Publishers, 2nd ed., 1997, pp. 1–18, 22, 158, 224, 284, 286–287, 293–296, 416–419, 453.

[2] P. Bacchin, P. Aimar and R.W. Field, Critical and sustainable fluxes: Theory, experiments and applications, J. Membr. Sci., 281 (2006) 42–69.

[3] S.S. Sablani, M.F.A. Goosen, R. Al-Belushi and M. Wilf, Concentration polarization in ultrafiltraion and reverse osmosis: a critical review, Desalination, 141 (2001) 269–289.

[4] M. Manttari and M. Nyström, Critical flux in NF of high molar mass polysaccharides and effluents from the paper industry, J. Membr. Sci., 170 (2000) 257–273.

[5] R.W. Field, D. Wu, J.A. Howell and B.B. Gupta, Critical flux concept for microfiltration fouling, J. Membr. Sci., 100 (1995) 259–272.

[6] R.J. Baker, A.G. Fane, C.D.J. Fell and B.H. Too, Factors affecting flux in crossflow filtration, Desalination, 53 (1985) 81–93.

[7] S.B. Sadr Ghayeni, S.S. Madaeni, A.G. Fane and R.P. Schineider, Aspects of microfiltration and reverse osmosis in municipal wastewater reuse, Desalination, 106 (1996) 25–29.

[8] J.A. Howell, Sub-critical flux operation of microfiltration, J. Membr. Sci., 107 (1995) 165–171.

[9] I.H. Huisman, The influence of membrane zeta potential on the critical flux for crossflow microfiltration particle suspensions, J. Membr. Sci., 156 (1999) 153–158.

[10] D.Y. Kwon, S. Vigneswaran, A.G. Fane and R. Ben Aim, Experimental determination of critical flux in cross-flow microfiltration, Separ. Purif. Technol., 19 (2000) 169–181.

[11] S. Metsamuuronen, J. Howell and M. Nyström, Critical flux in ultrafiltration of myoglobin and baker's yeast, J. Membr. Sci., 196 (2002) 13–25.

[12] H. Li, A.G. Fane, H.G.L. Coster and S. Vigneswaran, Direct observation of particle deposition on the membrane surface during crossflow microfiltration, J. Membr. Sci., 149 (1998) 83–97.

[13] D. Listsin, D. Hasson and R. Semiat, Critical flux detection in a silica scaling RO system, Desalination, 186 (2005) 311–318.

[14] S.S. Madaeni, The effect of operating conditions on critical flux in membrane filtration of latexes, Inst. Chem. Eng., Process Safety and Environmental Protection, 75 (1997) 266–269.

[15] J.S. Vrouwenvelder, J.A.M Paassen, J.M.C Agtmaal, M.C.M. Loosdrecht and J.C. Kruithof, A critical flux to avoid biofouling of spiral wound nanfiltration and reverse osmosis membranes: Fact or fiction?, J. Membr. Sci., 326 (2009) 36–44.

[16] W. Youravong, M.J. Lewis and S. Grandison, Critical flux in ultrafiltration of skimmed milk, J. IChem., 81 (2003) 303–308.

[17] I. Galambos, E. Csiszar, E.B. Molnar and G. Vatai, Mass transfer model for humic acid removal by ultrafiltration, Environ. Protect. Eng., 31 (2005) 145–152.

[18] J. Cho, G. Amy and J. Pellegrino, Membrane filtration of natural organic matter: initial comparison of rejection and flux decline characteristics with ultrafiltration and nanoiltration membranes, Wat. Res., 33 (1999) 2517–2526.

[19] R.F. Probstein, K.K. Chan, R. Cohen and I. Rubenstein, Model and preliminary experiments on membrane fouling in reverse osmosis, in Synthetic Membranes: Vol. 1, Desalination, A.F. Turbak, ed., Amer. Chem. Soc., Washington DC, 1981, pp. 131–145.

[20] A. Rubia, M. Rodriguez and D. Prats, pH, ionic strength and flow velocity effects on the NOM filtration with TiO_2/ZrO_2 membranes, Separ. Purif. Technol., 52 (2006) 325–331.